Laboratory Investigation (2017) 97, 1306–1320

Re-expression of *Sall1* in podocytes protects against adriamycin-induced nephrosis

Yoshiko Hosoe-Nagai[1], Teruo Hidaka[1], Ayano Sonoda[1], Yu Sasaki[1], Kanae Yamamoto-Nonaka[1,2], Takuto Seki[1,2], Rin Asao[1,2], Eriko Tanaka[1,3], Juan Alejandro Oliva Trejo[1,2,4], Fumiko Kodama[1], Miyuki Takagi[1], Nobuhiro Tada[5], Takashi Ueno[6], Ryuichi Nishinakamura[7], Yasuhiko Tomino[1] and Katsuhiko Asanuma[1,2]

The highly conserved spalt (sal) gene family members encode proteins characterized by multiple double zinc finger motifs of the C2H2 type. Humans and mice each have four known Sal-like genes (*SALL1–4* in humans and *Sall1–4* in mice). *Sall1* is known to have a crucial role in kidney development. To explore the significance of *Sall1* in differentiated podocytes, we investigated podocyte-specific *Sall1*-deficient mice (*Sall1* KO$^{p\alpha d\circ/p\alpha d\circ}$) using a podocin-Cre/loxP system and siRNA *Sall1* knockdown (*Sall1* KD) podocytes. Under physiological conditions, *Sall1* KO$^{p\alpha d\circ/p\alpha d\circ}$ mice exhibited no proteinuria during their lifetime, but foot-process effacement was detected in some of the podocytes. To elucidate the role of *Sall1* in injured podocytes, we used an adriamycin (ADR)-induced model of nephrosis and glomerulosclerosis. Surprisingly, the expression of *Sall1* was elevated in control mice on day 14 after ADR injection. On day 28 after ADR injection, *Sall1* KO$^{p\alpha d\circ/p\alpha d\circ}$ mice exhibited significantly higher levels of proteinuria and higher numbers of sclerotic glomeruli. Differentiated *Sall1* KD podocytes showed a loss of synaptopodin, suppressed stress fiber formation, and, ultimately, impaired directed cell migration. In addition, the loss of *Sall1* increased the number of apoptotic podocytes following ADR treatment. These results indicated that *Sall1* has a protective role in podocytes; thus, we investigated the endoplasmic reticulum stress marker GRP78. GRP78 expression was higher in ADR-treated *Sall1* KO$^{p\alpha d\circ/p\alpha d\circ}$ mice than in control mice. *Sall1* appeared to influence the expression of GRP78 in injured podocytes. These results suggest that *Sall1* is associated with actin reorganization, endoplasmic reticulum stress, and apoptosis in injured podocytes. These protective aspects of *Sall1* re-expression in injured podocytes may have the potential to reduce apoptosis and possibly glomerulosclerosis.

Laboratory Investigation (2017) **97,** 1306–1320; doi:10.1038/labinvest.2017.69; published online 31 July 2017

Podocyte foot processes (FP) and their interposed slit diaphragms (SD) are key components of the permeability barrier in glomeruli. Podocyte damage or loss can severely impair kidney function and is an early symptom of many kidney diseases involving nephrotic syndrome and/or glomerulosclerosis. Podocyte FP effacement and/or molecular reorganization of the SD are characteristic pathological features of nephrotic syndrome.[1] Elucidating the molecular mechanisms involved in the response of podocytes to damage is essential to understand podocyte pathogenesis.

The Spalt (sal) gene family encodes zinc finger proteins that both control normal development and apparently function as tumor suppressors in humans and mice.[2] *SALL1–SALL4* in humans have DNA sequence homologies with the Drosophila *sal* gene.[3] The Sall1 protein binds to A/T-rich sequences of the major satellite DNA via its C-terminal double zinc fingers, thereby localizing it to heterochromatin.[4] This protein also functions as a transcriptional repressor.[5] In humans, *SALL1* mutations cause an autosomal dominant disorder characterized by limb, ear, anus, heart, and kidney malformations.[6]

The importance of *Sall1* in kidney development has been investigated using *Sall1* knockout mice. Homozygous *Sall1* knockout mice die from kidney agenesis or severe dysgenesis within 24 h after birth.[7] *Sall1* is essential for ureteric bud

[1]Division of Nephrology, Department of Internal Medicine, Juntendo University Faculty of Medicine, Tokyo, Japan; [2]Laboratory for Kidney Research (TMK project), Medical Innovation Center, Kyoto University Graduate School of Medicine, Kyoto, Japan; [3]Department of Pediatrics, Tokyo Medical and Dental University, Tokyo, Japan; [4]Department of Cellular and Molecular Neuropathology, Juntendo University Graduate School of Medicine, Tokyo, Japan; [5]Atopy Research Center, Juntendo University School of Medicine, Tokyo, Japan; [6]Laboratory of Proteomics and Medical Science, Research Support Center, Juntendo University Faculty of Medicine, Tokyo, Japan and [7]Department of Kidney Development, Institute of Molecular Embryology and Genetics, Kumamoto University, Kumamoto, Japan
Correspondence: Dr K Asanuma MD, Laboratory for Kidney Research (TMK project), Medical Innovation Center, Kyoto University Graduate School of Medicine, 53 Shogoin Kawaharacho, Sakyo-ku, Kyoto 606-8397, Japan.
E-mail: asanuma@tmk.med.kyoto-u.ac.jp

Received 20 September 2016; revised 26 April 2017; accepted 1 May 2017

invasion and is required for the initial key step in metanephric development.[7] In the embryonic kidney, *Sall1* is highly expressed in mesenchyme-derived structures, including condensed mesenchyme, S-shaped bodies, comma-shaped bodies, renal tubules, and podocytes.[7] In a previous study, we generated podocyte-specific *Sall1* knockout mice (*Sall1* KO$^{Podo/Podo}$) to investigate the role of *Sall*1 after development.[8] In contrast to homozygous *Sall1* knockout mice, these mice were generated using the podocin promoter Cre-loxP system. Podocin is present in podocytes from the early capillary loop stage in developing nephrons and at the basal pole along the glomerular basement membrane (GBM) in mature glomeruli.[9] In the developing kidney, *Sall1* expression begins before the capillary loop stage, indicating that *Sall1* continues to be expressed until its suppression by the podocin promoter in podocyte-specific *Sall1* KO$^{Podo/Podo}$ mice.

In our previous study, we observed that the *Sall1* KO$^{Podo/Podo}$ mice showed no obvious phenotype under physiological conditions, with no significant difference in the level of urinary protein between wild-type (WT) and *Sall1* KO $^{Podo/Podo}$ mice, even beyond 48 h after the injection of lipopolysaccharide (LPS). Thus, this disease model exhibits minimal changes.[8] However, we also showed that LPS induces significant podocyte detachment from the GBM in these mice at 48 h after LPS injection.[8] Podocyte detachment from the GBM has been proven to cause progressive glomerulosclerosis and loss of kidney function.[10,11]

Adriamycin (ADR) treatment has been established as a model for nephrosis and focal segmental glomerular sclerosis (FSGS) in rats and mice.[12] Recent studies have used this model to elucidate some of the molecular details of kidney damage in ADR-induced nephrosis mice.[13–15] ADR induces podocyte apoptosis and loss of podocytes from the GBM, leading to glomerulosclerosis.[14,15]

Whether *Sall1* has a role in the pathogenesis of adult kidneys in conditions marked by severe nephrosis is unknown. To address this question, we used an ADR-induced mouse model of nephrotic syndrome to determine whether re-introduction of *Sall1* expression in injured podocytes causes reorganization of the actin cytoskeleton and apoptosis. We investigated the role and downstream effects of *Sall1* in injured podocytes.

MATERIALS AND METHODS

Antibodies

The following antibodies were used in immunohistochemistry and western blot analysis: monoclonal mouse anti-*Sall1* antibody (PPMX, Tokyo, Japan), polyclonal guinea pig anti-nephrin antibody (Progen, Heidelberg, Germany), polyclonal rabbit anti-WT1 antibody (Santa Cruz Biotechnology, Santa Cruz, CA, USA), monoclonal mouse anti-synaptopodin antibody (Progen, Heidelberg, Germany), monoclonal mouse anti-GAPDH antibody (Abcam, Cambridge, UK), monoclonal rabbit anti-glucose-regulated protein 78 antibody (Cell Signaling Technology, Beverly, MA, USA), and polyclonal rabbit anti-cleaved caspase 3 antibody (Cell Signaling Technology, Beverly, MA, USA). Polyclonal rabbit anti-podocin antibody and polyclonal rabbit anti-synaptopodin antibody have been described previously.[16]

Mouse Models

We mated *Sall1* floxed mice (*Sall1*$^{flox/flox}$) with podocin-*Cre* mice to generate *Sall1* KO$^{Podo/Podo}$ mice.[17,18] Transgenic mice (*Sall1* floxed mice, *Sall1*$^{flox/flox}$) were obtained from the Department of Kidney Development, Institute of Molecular Embryology and Genetics, Kumamoto University, Japan.[18] Podocin-Cre mice have been previously described.[17] *Sall1* KO$^{Podo/Podo}$ mice were backcrossed onto a BALB/c background (>12 generations). Podocin-*Cre*-negative *Sall1*$^{flox/flox}$ littermates were used as control animals.

We used *Sall1* KO $^{Podo/Podo}$ mice weighing ~ 30 g at 12 weeks of age for ADR (doxorubicin hydrochloride; Wako, Osaka, Japan)-induced nephropathy. All mice in this experiment had a BALB/c background. Proteinuria was induced via tail vein injection of ADR diluted with 0.9% saline.[15] A low dose of ADR (8 mg/kg body weight) was used in the control mice group to induce proteinuria with only a few sclerotic glomeruli. We did not use the high dose of ADR (13 mg/kg body weight) used in our previous study because it caused high rates of death in *Sall1* KO$^{Podo/Podo}$ mice.

ADR was injected into littermate control mice. The urinary albumin/creatinine ratio (ACR) was measured using an immunoassay (DCA 2000 systems; Siemens Medical Solutions Diagnostics, Munich, Germany) with a Bayer DCA 2000+ chemical analyzer (Bayer Diagnostics, Elkhart, USA).[19] Using pentobarbital sodium (100 mg/kg body weight) (Dainippon Sumitomo Pharma, Osaka, Japan) for anesthesia, 4–8 mice were sacrificed on days 0, 7, 14, 21, and 28 after ADR injection. Specific pathogen-free conditions prevented infections.

All animal handling and experiments were performed strictly in accordance with the recommendations of the guidelines for the Care and Use of Laboratory Animals of the Juntendo University Faculty of Medicine. The experimental protocol was approved by the Animal Care and Use Committee of Juntendo University, Tokyo, Japan.

Cell Culture and Transient Transfection

The conditionally immortalized murine podocyte cell lines have been described previously.[20] To evaluate the reaction to ADR *in vitro*, cells were treated with 0.2 μg/ml of ADR in regular medium; the medium was refreshed at 24 h after ADR treatment. Immunofluorescence (IF) microscopy of the cultured podocytes was performed as described previously.[16]

Stable gene silencing of *Sall1* in podocytes was performed using pSUPER system as described previously.[21] The *Sall1*-specific insert used the following 19-nucleotide sequence: 5-GCCTGAAGTCTGTGGAGAA-3. Stable clonal populations of siRNA knockdown podocyte cell lines were

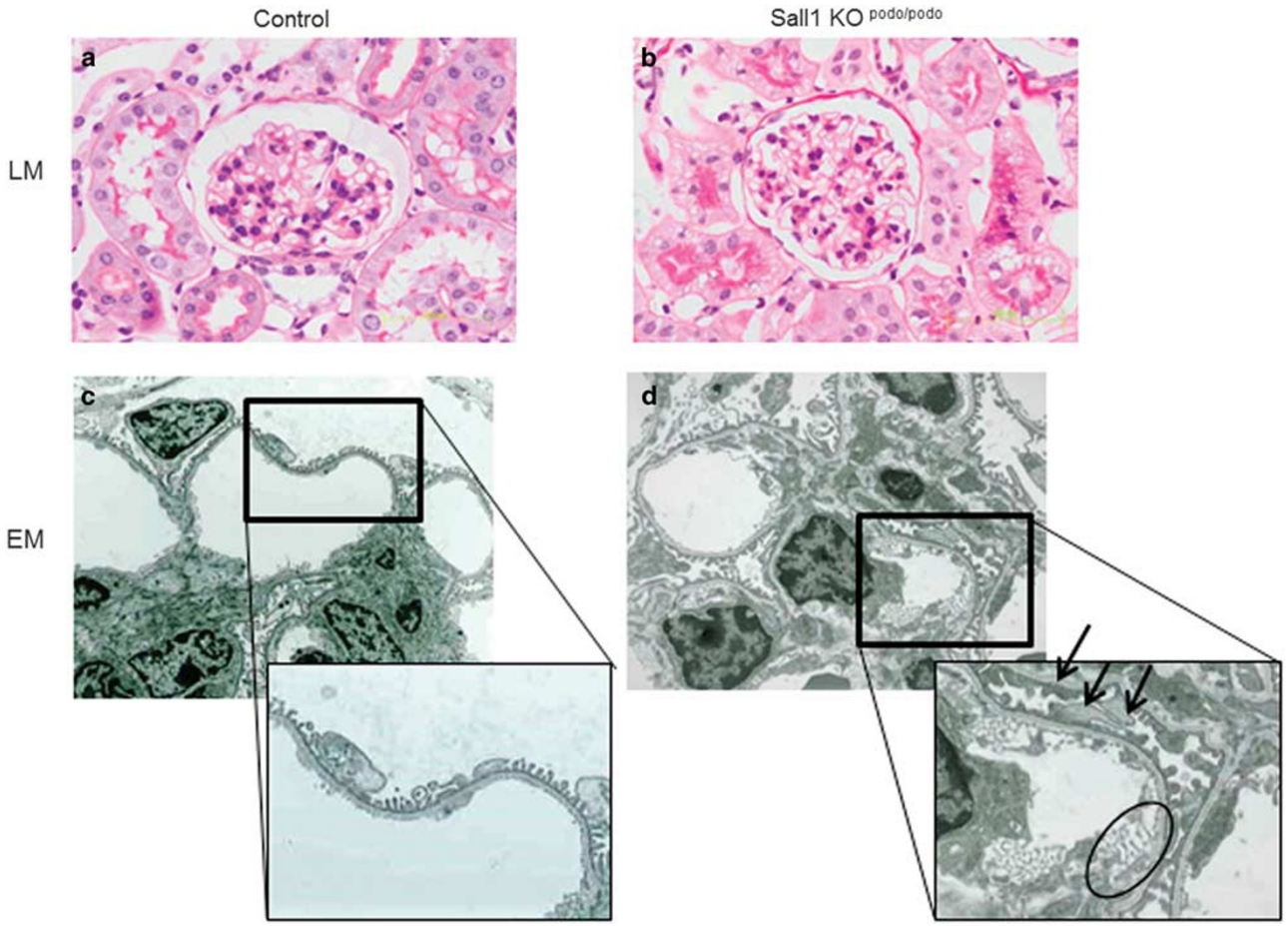

Figure 1 The phenotype of podocyte-specific *Sall1* KO mice under physiological conditions. (**a**,**b**) Periodic acid–Schiff staining images of kidney sections showing normal glomeruli and tubules in both WT littermate mice (**a**) and 12-week-old *Sall1* KO $^{podo/podo}$ mice (**b**) on LM (original magnification, 400×). (**c**) No FP effacement is observed in control glomeruli on EM (original magnifications: lower, 3000×; higher, 8000×). (**d**) Glomeruli in *Sall1* KO$^{podo/podo}$ mice exhibit FP effacement (arrows) and arcade formation of endothelial cells (circles) on EM (original magnifications: lower, 3000×; higher, 8000×).

established. We used randomized siRNA (a control vector pSUPER)-transfected podocytes as a control.[21]

Renal Histology and Immunohistochemistry

Mouse kidneys were removed, fixed by perfusion with 4% paraformaldehyde in phosphate-buffered saline (PBS), perfused with a cryoprotectant (20% sucrose in PBS) and embedded in paraffin for light microscopy and morphometric analysis of glomerulosclerosis and interstitial fibrosis. For the histological study, 3-μm thick kidney sections were stained with periodic acid–Schiff (PAS) reagent or Azan–Mallory staining to examine interstitial fibrosis. Blue-stained interstitial fibrotic areas were carefully observed in each tissue section. These sections were observed under the light microscope (Olympus BX41; Olympus, Tokyo, Japan).[15] At least 200 glomeruli were randomly selected for determination of glomerulosclerosis. Glomeruli that exhibited adhesion of the capillary tuft to Bowman's capsule, capillary obliteration, mesangial expansion, or fibrotic crescents were defined as glomerulosclerotic.[22] Sclerotic glomeruli per section were assessed using a total number count, as described previously.[15]

For the immunofluorescence study, fixed kidneys were frozen in an optimal cutting temperature compound. Frozen sections (4–5 μm) were immunostained with primary antibodies followed by the respective secondary antibodies, as described previously.[15] We randomly examined >100 glomeruli in each experimental group to determine the number of cells double-positive for WT1 and 4′,6-diamidino-2-phenylindole (DAPI) and calculated the average. To obtain further morphological information, sections were analyzed by electron microscopy (EM) using an electron microscope (H-7100; Hitachi, Tokyo, Japan) at 75 kV as described previously.[15]

For the immunohistochemical study, slides of kidney cortex samples from mice were dewaxed, washed with PBS, and subjected to microwave heating at 600 W for 15 min for antigen retrieval. The slides were incubated with 1.3%

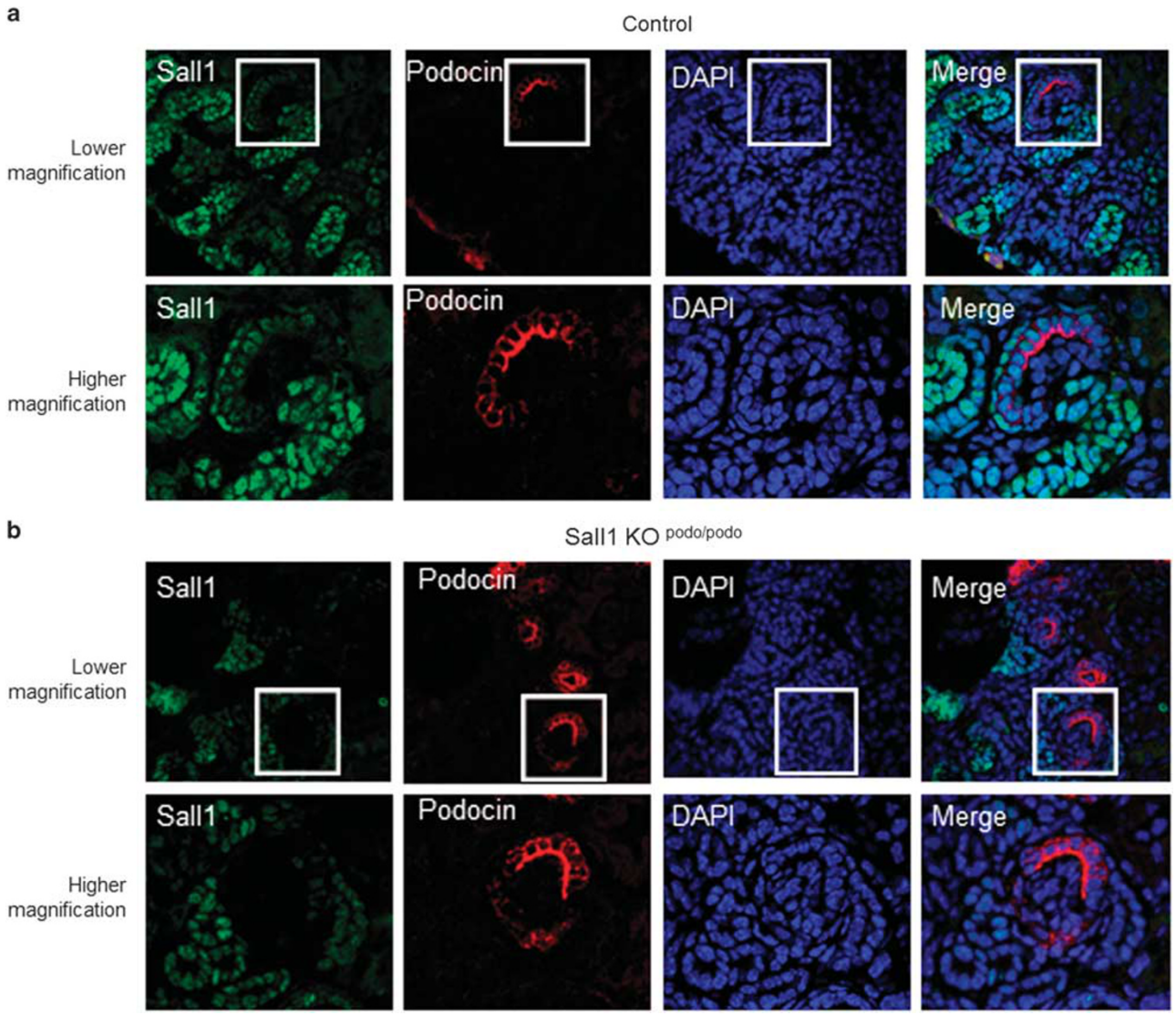

Figure 2 (**a**) Control mice, (**b**) *Sall1* KO $^{podo/podo}$. Expression of *Sall1* is lost in the early capillary stages of the developing kidneys of 2-day-old mice and is simply driven by a podocin promoter in the *Sall1* KO$^{podo/podo}$ mice (original magnifications: lower, 400×; higher, 1000×).

H_2O_2/Tris-buffered saline (TBS) for 15 min and then treated with blocking buffer (3% bovine serum albumin and 0.05% Tween-20 in TBS) for 60 min. The slides were then incubated with anti-*Sall1* antibody at 4 °C overnight. Immune complexes were detected using a DAB substrate solution kit (Histofine Mouse Stain kit and DAB substrate solution kit; Nichirei Bioscience, Tokyo, Japan). The enzyme-labeled antibodies method was used to detect *Sall1* in ADR-injected mice.

Western Blot Analysis

Mouse glomeruli were isolated from the kidneys using a graded sieving method, as described previously.[23] Isolated glomeruli were lysed, and western blot analysis was performed as described previously.[23] Membranes were incubated with the primary antibodies overnight at 4 °C. After washing with 0.05% Tween-20 in TBS, membranes were incubated with either horseradish peroxidase-labeled goat anti-rabbit immunoglobulin (Ig)G antibody or anti-mouse IgG antibody, and labeling was detected using a Western Lightning Chemiluminescence Reagent Kit (Life Science Products, Boston, MA, USA). GAPDH was used as the internal control.

Wound-Healing Assay

Wound-healing assays were performed as described previously,[24] with some modifications. Differentiated control podocytes and *Sall1* knockdown (KD) podocytes (5×10^5) were seeded into six-well plates and wounded with a 200-μl pipette tip. The wounded monolayers were washed with PBS and incubated in Roswell Park Memorial Institute 1640 medium. Time-lapse images were taken using a 10× phase

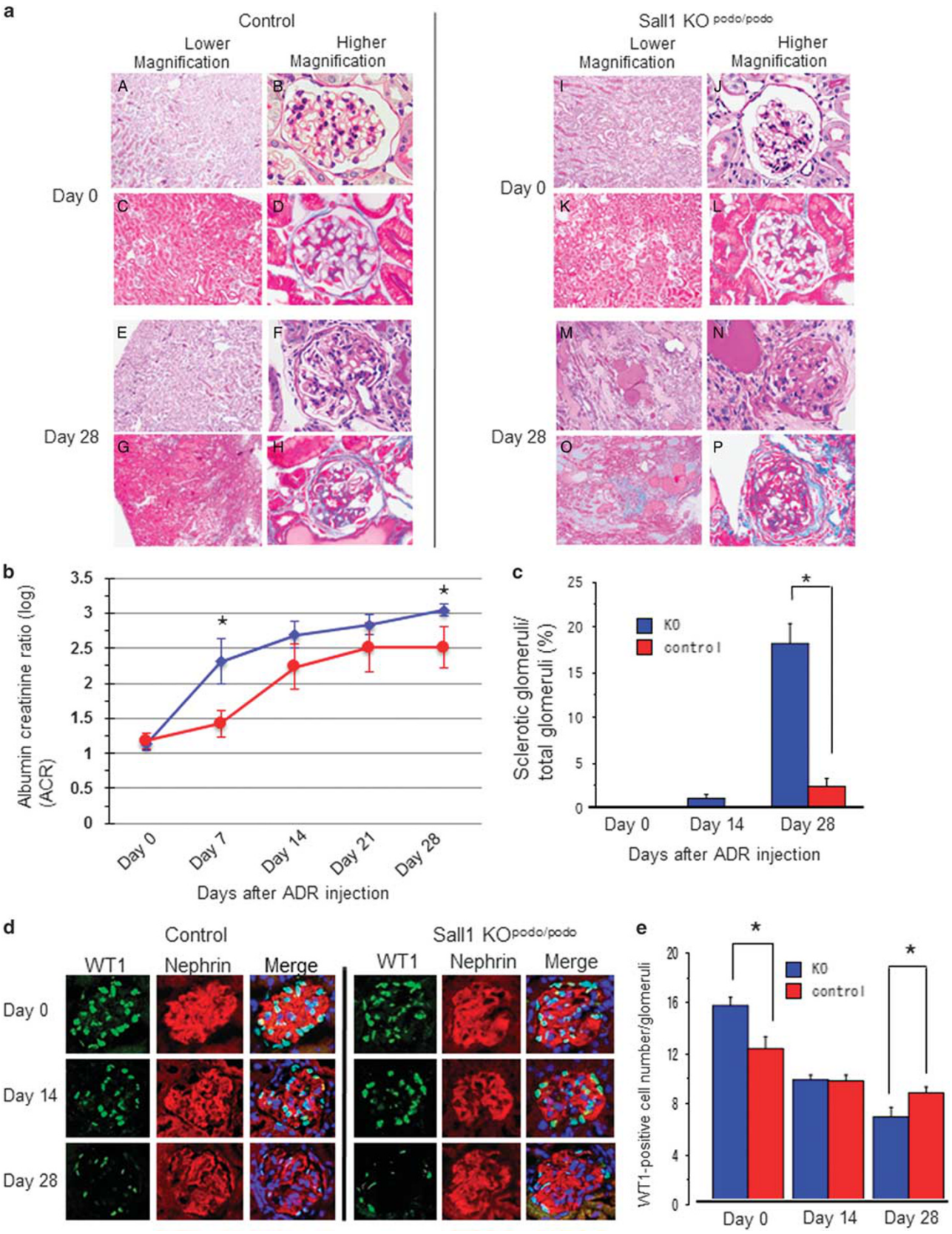
a
Control
Lower Magnification
Higher Magnification
Sall1 KO podo/podo
Day 0
Day 28
A
B
C
D
E
F
G
H
I
J
K
L
M
N
O
P
b
Albumin creatinine ratio (log) (ACR)
3.5
3
2.5
2
1.5
1
0.5
0
Day 0
Day 7
Day 14
Day 21
Day 28
Days after ADR injection
*
c
Sclerotic glomeruli/ total glomeruli (%)
25
20
15
10
5
0
KO
control
Day 0
Day 14
Day 28
Days after ADR injection
d
Control
Sall1 KOpodo/podo
WT1
Nephrin
Merge
Day 0
Day 14
Day 28
e
WT1-positive cell number/glomeruli
20
16
12
8
4
0
KO
control
Day 0
Day 14
Day 28

contrast objective and an All-in-One Fluorescence Microscope (Keyence, Osaka, Japan) at 0, 12, and 24 h. At the indicated time points, monolayers were photographed using the grid as a marker, and the wound width (μm) was measured at each time point using the All-in-One software (Keyence). Migratory rates were calculated as $(A-B)/A\times 100\%$ and $(A-C)/A\times 100\%$, with A, B, and C representing the width of the wound at 0, 12, and 24 h, respectively. Data are presented as the mean ± s.e. of five independent experiments.

Cell Migration and Apoptosis Assays

Differentiated control and *Sall1* KD podocytes (7×10^5 each) were added to a 24-well migration plate (Cell Biolabs, CA, USA). Migration assays were performed for 24 h, and the upper insert was removed. Cells on the bottom of each well were stained with crystal violet staining solution (Sigma-Aldrich, MO, USA), and the number of stained cells was counted.

To detect apoptotic cells *in vivo*, an Apop Tag Plus Peroxidase *in vivo* Apoptosis Detection Kit (Chemicon international, Temecula, California, USA) was purchased for the TdT-mediated dUTP nick end-labeling (TUNEL) assay. TUNEL-positive cells in the nonsclerotic parts of the glomeruli were counted as described previously.[15]

Measurement of Apoptosis by Annexin V and Propidium Iodide

Cells (6×10^5) were treated with 0.15 μg/ml of ADR for 48 h and then washed and suspended in a binding solution containing annexin V-FITC at dilutions recommended by the manufacturer's protocol (BioVision, Milpitas, CA, USA). After 20 min, propidium iodide (PI; 1 μg/ml) was added. At least 10 000 cells per sample were analyzed using fluorescence-activated cell sorting. Early and late apoptosis were determined as percentages of annexin V+/PI− and annexin V+/PI+ cells, respectively.

Statistical Analysis

Quantification of western blots was performed using image-processing software (Image J). Data are presented as the mean ± s.e. Urinary protein data were log-transformed before statistical analysis to stabilize the variance. Student's *t*-test was used to analyze differences between the two groups. Analysis of repeat *t*-tests, followed by Bonferroni correction, was used when more than two groups were compared. All experiments were repeated at least three times, and representative experiments are shown. Two-factor repeated measures analysis of variance (ANOVA) was used when there were two or more dependent variables. Differences were regarded as significant at $P<0.05$.

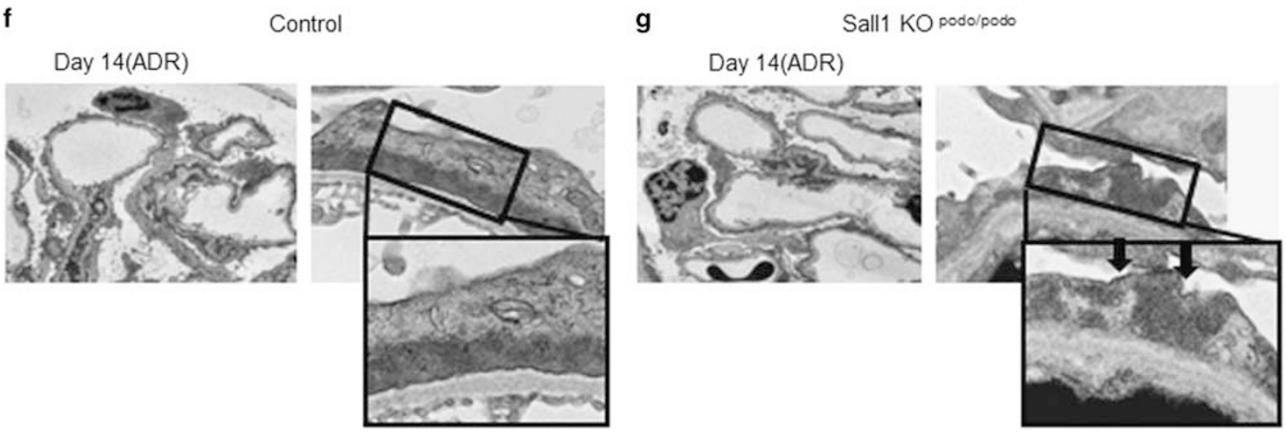

Figure 3 Continued.

Figure 3 ADR injection causes heavy proteinuria and glomerulosclerosis in the *Sall1* KO$^{podo/podo}$ mice. (**a**) The number of sclerotic glomeruli and area of interstitial fibrosis are greatly increased in *Sall1* KO$^{podo/podo}$ mice on day 28 after ADR injection. The area of interstitial fibrosis is stained blue with Azan–Mallory staining. PAS staining (**A**, **B**, **E**, **F**, **I**, **J**, **M**, **N**); Azan–Mallory staining (**C**, **D**, **G**, **H**, **K**, **L**, **O**, **P**) (lower magnification, 400×; higher magnification, 1000×). (**b**) Levels of urinary protein are significantly increased in *Sall1* KO$^{podo/podo}$ mice on days 7 and 28 ($P<0.05$; $n=8$). (**c**) The sclerotic glomeruli/total glomeruli ratio is significantly higher in *Sall1* KO$^{podo/podo}$ mice than in control mice on day 28 ($P<0.05$; 300 glomeruli each in $n=5$). (**d**) Mean podocyte numbers per nonsclerotic glomeruli on days 0, 14, and 28 are shown for cells double-positive for WT1 and DAPI. Magnification, 600×. (**e**) Before ADR injection, the number of podocytes (WT1-positive cells) in *Sall1* KO$^{podo/podo}$ mice is higher than that in control mice ($P<0.05$; 100 glomeruli each in $n=3$). On day 28 after ADR injection, the number of podocytes in *Sall1* KO$^{podo/podo}$ mice is significantly lower than that of control mice ($P<0.05$; 100 glomeruli each in $n=3$). (**f**) Podocytes in control mice 14 days after ADR injection exhibit FP effacement on the GBM. (**g**) Podocytes in *Sall1* KO$^{podo/podo}$ mice 14 days after ADR injection exhibit larger areas of FP effacement and irregular actin accumulation (arrows) (original magnifications: lower, 3000×; higher, 12 000×).

RESULTS

Phenotype of Podocyte-Specific *Sall1* KO Mice

There were no significant differences in body weight between the podocyte-specific *Sall1* KO mice groups at any time point (Supplementary Figure 1). Urinary protein tests were negative during the 2.5 years (data not shown).

There were no obvious histological abnormalities in the 12-week-old *Sall1* KO$^{pod\text{-}o/pod\text{-}o}$ mice by LM (Figure 1a and b). To examine morphology in detail, we performed EM. Glomeruli in the *Sall1* KO$^{pod\text{-}o/pod\text{-}o}$ mice partially showed FP effacement and arcade formation of the endothelial cells (Figure 1c and d). Arcade formation of the endothelial cells has been found to show cellular hypertrophy induced by endothelial injury ultrastructurally.[25] In acute glomerular lesions, dissociation of endothelial cells from the GBM was observed in association with subendothelial edema, which is recognized as arcade formation.[26]

We studied FP effacement by quantitating the FP width and examined arcade formation by endothelial cells as a marker of endothelial cellular hypertrophy induced by injury to the endothelial ultrastructure. For each glomerulus, the average percentage of GBM length with arcade formation was calculated via division of the total length of arcade formation by the total length of the GBM. No significant differences were observed, but the results showed a tendency to increase FP effacement and arcade formation in the *Sall1* KO$^{pod\text{-}o/pod\text{-}o}$ mice (Supplementary Figure 2).

We investigated *Sall1* expression in the developing kidneys of 2-day-old mice via immunofluorescence microscopy. Expression of *Sall1* was still observed in podocytes in the early capillary stages of developing kidneys in the control mice (Figure 2a). In contrast, expression of *Sall1* was lost in the podocytes of *Sall1* KO $^{pod\text{-}o/pod\text{-}o}$ mice (Figure 2b).

ADR Injection Caused Heavy Proteinuria and Glomerulosclerosis in *Sall1* KO $^{pod\text{-}o/pod\text{-}o}$ Mice

To elucidate the role of *Sall1* in injured podocytes, we used an ADR-induced nephrosis model. On day 7, partial glomerulosclerosis and expansion of the mesangial area appeared in the ADR-injected *Sall1* KO$^{pod\text{-}o/pod\text{-}o}$ mice (data not shown). *Sall1* KO$^{pod\text{-}o/pod\text{-}o}$ mice developed even more glomerulosclerosis and interstitial fibrosis on day 28 (Figure 3a,M-P). Urinary ACR levels were significantly elevated in *Sall1* KO$^{pod\text{-}o/pod\text{-}o}$ mice on day 7 (ACR [log]: *Sall1* KO$^{pod\text{-}o/pod\text{-}o}$ mice *vs* control mice, 2.3 ± 0.3 *vs* 1.4 ± 0.2; $P < 0.05$; $n = 8$) and on day 28 (3.0 ± 0.1 *vs* 2.5 ± 0.3, respectively; $P < 0.05$; $n = 8$) (Figure 3b). Hematuria was not observed in either group during the experimental period. On day 28, the sclerotic glomeruli/total glomeruli ratio was significantly higher in *Sall1* KO$^{pod\text{-}o/pod\text{-}o}$ mice than in control mice (*Sall1* KO$^{pod\text{-}o/pod\text{-}o}$ *vs* control mice, 17.3 ± 1.9 *vs* $2.0 \pm 1.0\%$, respectively; $P < 0.05$; 300 glomeruli each in $n = 5$) (Figure 3c).

To count the number of podocytes on the GBM, double-positive cells for WT1 and DAPI were counted in nonsclerotic glomeruli (Figure 3d). Before ADR injection, the number of podocytes (WT1-positive cells) was greater in *Sall1* KO$^{pod\text{-}o/pod\text{-}o}$ mice than in control mice (16.9 ± 0.7 *vs* 13.1 ± 1.1, respectively; $P < 0.01$; 100 glomeruli each in $n = 3$) (Figure 3e). Podocyte loss was detected from day 14. On day 28 after ADR injection, the number of podocytes (WT1-positive cells) in *Sall1* KO$^{pod\text{-}o/pod\text{-}o}$ mice had significantly decreased compared with that of control mice (7.2 ± 0.8 *vs* 9.3 ± 0.5, respectively; $P < 0.05$; 100 glomeruli each in $n = 3$) (Figure 3e).

To further address the differences in glomerular abnormalities between control and *Sall1* KO$^{pod\text{-}o/pod\text{-}o}$ mice, we used transmission EM to examine the glomerular ultrastructure (Figure 3f and g). In both control and *Sall1* KO$^{pod\text{-}o/pod\text{-}o}$ mice, FP effacement was detected on podocytes 14 days after ADR injection. Podocytes in control mice showed dark-staining actin belts on the GBM (Figure 3f). In contrast, podocytes in *Sall1* KO$^{pod\text{-}o/pod\text{-}o}$ mice showed irregular actin accumulation (Figure 3g).

Expression of *Sall1* Significantly Increased in Control Glomeruli After ADR Injection

To check *Sall1* expression in injured podocytes, we immunostained *Sall1* in tissue samples (Figure 4a). Expression of *Sall1* was significantly elevated on day 14 after ADR injection in control mice. On day 7 and thereafter, expression of *Sall1* was elevated in the glomeruli of the ADR-injected control

Figure 4 *Sall1* expression significantly increases on day 14 after ADR injection. (**a**) By immunohistochemical analysis, *Sall1* expression is increased in the glomeruli of ADR-injected control mice on day 7 and thereafter. Expression of *Sall1* is absent in *Sall1* KO$^{pod\text{-}o/pod\text{-}o}$ mice. Magnification, 600×. (**b**) Immunohistochemical analysis of *Sall1* immunoreactivity. Expression of *Sall1* is significantly elevated on day 14 after ADR injection in control mice. (**c**,**d**) Western blot analysis shows that *Sall1* expression is significantly elevated on day 14 after ADR injection in control mice ($P < 0.05$; $n = 5$). The molecular weights of *Sall1* and GAPDH proteins are 140 and 40.2 kDa, respectively. To verify the expression level objectively, we measured bands using Image J, and the correction was performed by GAPDH. (**e**) Western blot analysis shows that *Sall1* expression is very low in *Sall1* KO$^{pod\text{-}o/pod\text{-}o}$ mice. (**f**) TUNEL staining to detect apoptotic cells *in vivo*. The number of TUNEL-positive cells in the nonsclerotic glomeruli is significantly increased in the *Sall1* KO$^{pod\text{-}o/pod\text{-}o}$ mice on day 14 (counted TUNEL-positive cells/total nonsclerotic glomeruli of control mice *vs* *Sall1* KO$^{pod\text{-}o/pod\text{-}o}$ mice; $P < 0.05$; $n = 8$). (**g**) To identify TUNEL-positive cells, we stained serial sections of the TUNEL assay samples. Positive cells (red arrow) are positive for synaptopodin in ADR-injured *Sall1* KO$^{pod\text{-}o/pod\text{-}o}$ mice (day 14). (**h**) TUNEL-positive cells in the glomeruli of ADR-injected Sall1 KO$^{pod\text{-}o/pod\text{-}o}$ mice (day 14). (**i**) Western blot analysis of cleaved caspase 3 to confirm podocyte apoptosis at the protein level in ADR-injured WT mice and *Sall1* KO$^{pod\text{-}o/pod\text{-}o}$ mice. Image J was used as in Figure 4d. Bands were adjusted to control as 100. In WT mice, the level of cleaved caspase 3 increased on day 14 and decreased on day 28. In *Sall1* KO$^{pod\text{-}o/pod\text{-}o}$ mice, cleaved caspase 3 was present even on day 0, increased on day 14, and decreased on day 28.

mice (Figure 4b). On western blot analysis, expression of *Sall1* was significantly elevated in the glomeruli on day 14 after ADR injection (Figure 4c and d). In *Sall1* KO $^{podo/podo}$ mice, expression of *Sall1* was not detected during the experiments (Figure 4a and e).

We previously reported that ADR-induced nephropathic mice showed an increased number of apoptotic podocytes, leading to glomerulosclerosis.[15] To detect apoptotic cells *in vivo*, TUNEL staining was performed. The ratio of TUNEL-positive cells to total nonsclerotic glomeruli was significantly

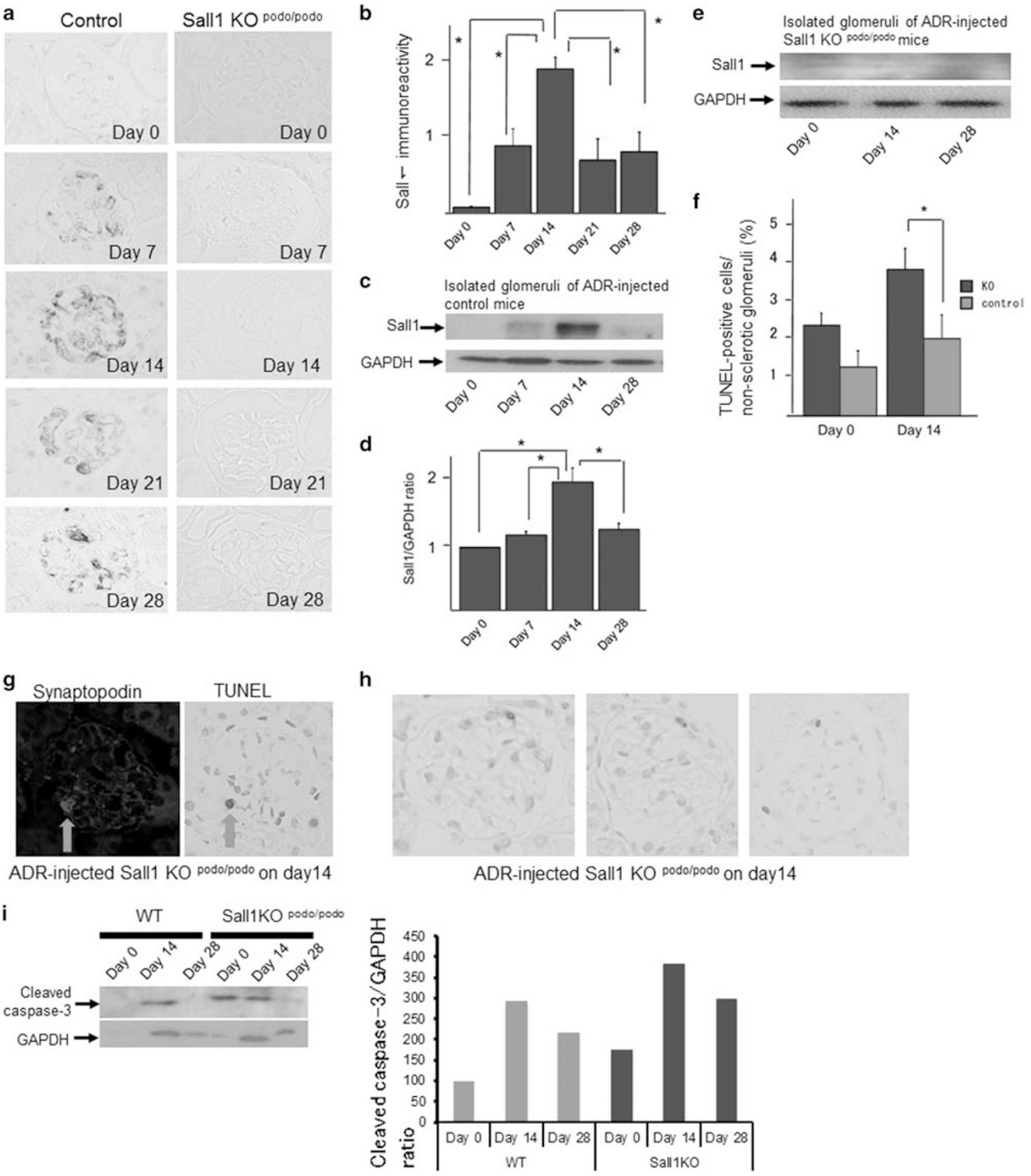

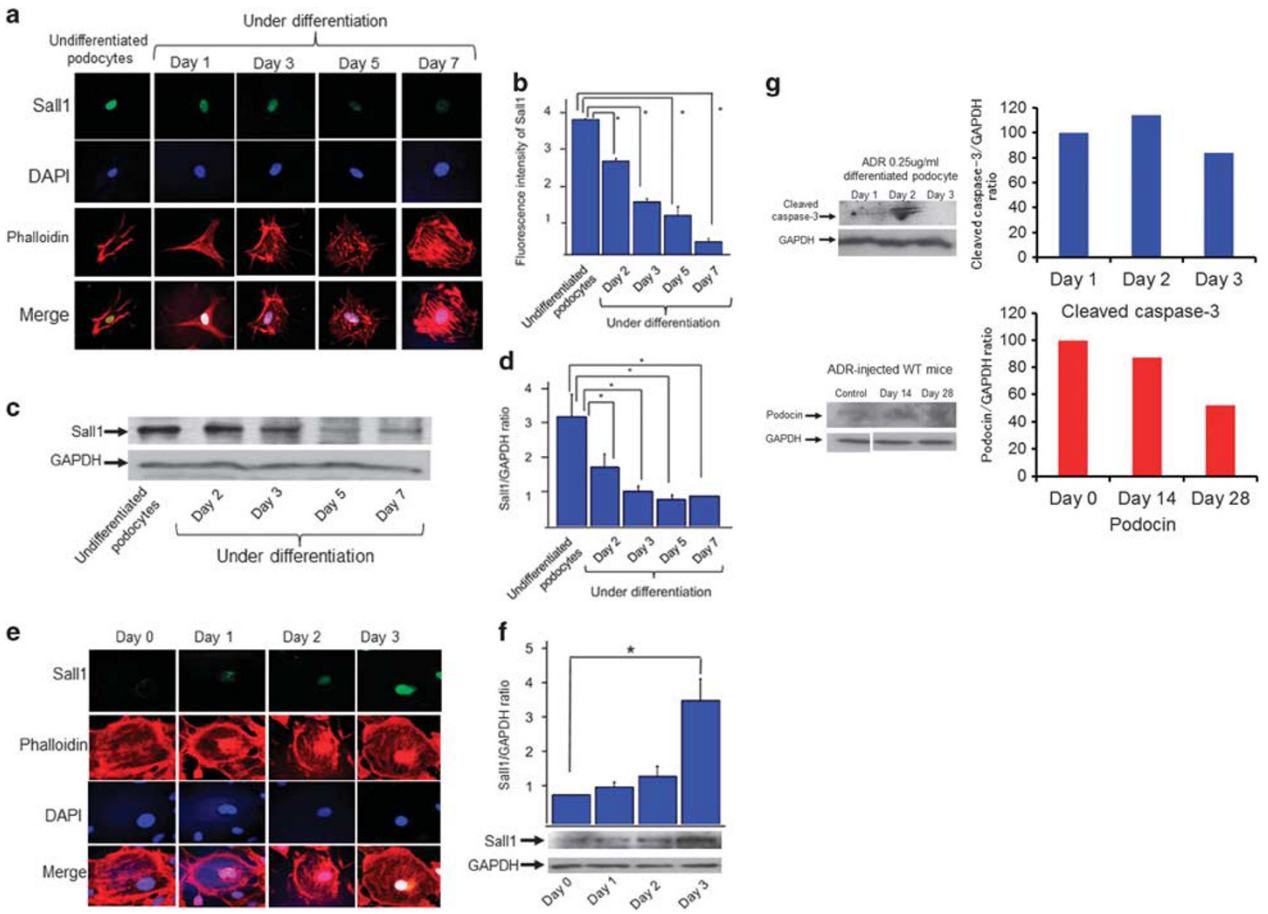

Figure 5 Expression of *Sall1* is elevated on day 3 after ADR treatment in cultured differentiated podocytes. (**a**) IF microscopy clearly shows that *Sall1* expression in undifferentiated podocytes overlaps with DAPI staining. *Sall1* expression in cultured podocytes gradually decreases with differentiation (original magnification, 1000×). (**b**) Confocal microscopy results analyzed for fluorescence intensity of *Sall1* are presented in the bar graph. *Sall1* expression is significantly lower in differentiated than in undifferentiated podocytes (*$P<0.05$; $n=5$). (**c**,**d**) Western blot analysis shows that expression of *Sall1* in differentiated podocytes is significantly reduced (*$P<0.05$; $n=5$). (**e**) Differentiated podocytes were treated with 0.2 μg/ml of ADR for 24 h. On days 1 and 2 after ADR treatment, *Sall1* expression is not detectable, and stress fibers are decreased in the differentiated podocytes. On day 3 after ADR treatment, *Sall1* expression increased in the nuclei of podocytes, and the reproduction of stress fibers is detected. (**f**) Western blot analysis shows that *Sall1* expression is significantly elevated on day 3 after ADR treatment in differentiated podocytes (*$P<0.05$; $n=5$). (**g**) Cleaved caspase 3 in ADR-treated, differentiated podocytes. The level of cleaved caspase 3 is higher on day 2 and lower on day 3 relative to that on day 1. Image J software was used for analysis as in Figure 4d. Bar graph compares levels of cleaved caspase 3 relative to that on day 1, which is set as 100. To evaluate podocyte injury at the protein level, we measured the expression of podocin in ADR-injected WT mice. After ADR injection, the expression of podocin gradually decreased.

higher in *Sall1* KO$^{pod\alpha/pod\alpha}$ mice on day 14 relative to that of control mice. (*Sall1* KO$^{pod\alpha/pod\alpha}$ *vs* control mice, 3.3 ± 0.4 *vs* $1.3\pm0.5\%$, respectively; $P<0.05$; $n=8$) (Figure 4f).

To determine whether the TUNEL-positive cells were podocytes, we stained the cells simultaneously with synaptopodin. The same cells were positive in the TUNEL assay and synaptopodin immunofluorescence staining (Figure 4g and h).

To evaluate podocyte apoptotic damage, we measured cleaved caspase 3 levels in ADR-treated cells *in vivo*. The level of cleaved caspase 3 in WT mice increased after ADR treatment. Interestingly, in *Sall1* KO$^{pod\alpha/pod\alpha}$ mice, cleaved caspase 3 was elevated both before and after ADR treatment (Figure 4i). Surprisingly, on day 28 after ADR treatment, this expression decreased in both WT and *Sall1* KO$^{pod\alpha/pod\alpha}$ mice (Figure 4i).

Expression of *Sall1* Increased After ADR Treatment in Cultured Differentiated Podocytes

To elucidate the role of *Sall1 in vitro* under pathological conditions, we used a cultured murine podocyte cell line.[20] On IF staining, the expression of *Sall1* gradually decreased and correlated with podocyte differentiation (Figure 5a). *Sall1* expression significantly decreased day by day under differentiation as determined by fluorescent intensity (Figure 5b). To confirm the expression of *Sall1* in cultured podocytes during differentiation, western blot analysis was performed. The expression of *Sall1* in differentiated podocytes was significantly lower than in undifferentiated podocytes (Figure 5c and d).

To investigate the levels of *Sall1* in injured podocytes, we further examined the expression of *Sall1* in differentiated

ADR-treated podocytes. After ADR treatment (0.2 μg/ml), *Sall1* expression remained low on days 1 and 2. On day 3, *Sall1* expression increased significantly (Figure 5e and f). Analysis of actin stress fibers showed that they were lost, with the exception of cortical actin, on day 1 after ADR treatment. On days 2 and 3, however, actin stress fibers were replenished (Figure 5e).

Similar to the *in vivo* study, we measured cleaved caspase 3 expression in differentiated ADR-treated podocytes *in vitro*. After ADR treatment (0.25 μg/ml), podocytes expressed cleaved caspase 3 on days 1 and 2 (Figure 5g, upper panel), with greater expression on day 2 than on day 1. However, for unknown reasons, this expression decreased on day 3. Despite this decrease, *Sall1* may prevent podocyte damage. Further experiments are required to study this potential action of *Sall1* more thoroughly.

Sall1 KD in Cultured ADR-treated Podocytes Resulted in Loss of Actin Stress Fiber Formation Under Differentiation and Increased Apoptotic Damage

To explore the role of *Sall1* in injured podocytes, we generated *Sall11* KD podocytes. Western blot analysis of *Sall1* was performed after gene silencing by the stable expression of a *Sall1*-specific siRNA in undifferentiated podocytes, and stable *Sall1* KD podocytes showed an almost complete loss of *Sall1* protein expression (Figure 6a). Differentiated WT podocytes showed increased cell body size, with an arborized appearance (Figure 6b). In contrast, the size of podocyte cell bodies was barely increased under differentiated conditions in *Sall1* KD podocytes (Figure 6b).

Synaptopodin is an actin-associated protein that may have a role in actin-based cell shape and motility in podocytes.[22,24,27] We hypothesized that *Sall1* regulates stress fiber formation and cell motility promoted by synaptopodin. In western blot analysis, no synaptopodin expression was observed in undifferentiated WT and *Sall1* KD podocytes (Figure 6c). Synaptopodin expression was significantly lower in differentiated *Sall1* KD podocytes than in differentiated WT podocytes (Figure 6c). Glomerular synaptopodin is highly unstable, and its decomposition generates a 44-kDa fragment;[24] however, there were no differences in synaptopodin degradation between the two cell types (Figure 6c). Synaptopodin was located in differentiated WT podocytes in a typical pattern of stress fibers (Figure 6d). The abundance of stress fibers was lower in differentiated *Sall1* KD podocytes (Figure 6d).

To examine whether the expression of *Sall1* regulates podocyte migration, wound-healing and migration assays were performed. *Sall1* KD podocytes significantly inhibited directional podocyte migration at 24 h (WT *vs Sall1* KD podocytes, 99.8 ± 0.2 *vs* $73.9 \pm 0.5\%$, respectively; $P = 0.0001$; $n = 5$) (Figure 6e). *Sall1* KD podocytes were significantly less motile than were WT podocytes (WT *vs Sall1* KD podocytes: 173.6 ± 11.9 cells *vs* 126.8 ± 7.6 cells, respectively; $P < 0.05$; $n = 5$) (Figure 6f).

We previously showed that ADR treatment directly caused podocyte apoptosis *in vitro*.[15] Measurement of apoptosis by annexin V and PI staining showed that ADR treatment induced severe apoptosis in *Sall1* KD podocytes (number of early apoptotic WT podocytes *vs Sall1* KD podocytes: 2.1 ± 0.3 *vs* $7.9 \pm 0.8\%$, respectively; $P < 0.01$) (number of late apoptotic WT podocytes *vs Sall1* KD podocytes: 3.1 ± 0.3 *vs* $6.1 \pm 0.2\%$, respectively; $P < 0.01$, $n = 5$) (Figure 6g).

Endoplasmic Reticulum Stress is Increased in ADR-injected *Sall1* KO$^{Pod\circ/Pod\circ}$ Mice

The 78-kDa glucose-regulated protein (GRP78), which is a key molecular chaperone stimulated by ER stress, is upregulated in podocytes and is involved in the movement of nephrin from SDs to cell bodies.[28] In ADR-injected control and *Sall1* KO$^{Pod\circ/Pod\circ}$ mice, low-level expression of GRP78 was detected by immunofluorescence staining from day 7, with a gradual increase until day 28 (Figure 7a and b). On day 28, the expression of GRP78 was significantly higher in ADR-injected *Sall1* KO$^{Pod\circ/Pod\circ}$ mice than in ADR-treated control mice (Figure 7c).

DISCUSSION

We investigated the role of *Sall1* in injured podocytes using an ADR-induced model of nephrosis and glomerulosclerosis. Significantly higher levels of proteinuria and higher numbers of sclerotic glomeruli were detected in *Sall1* KO$^{Pod\circ/Pod\circ}$ mice than in controls by 28 days after ADR treatment. Differentiated *Sall1* KD podocytes showed a loss of synaptopodin, suppressed stress fiber formation, and, ultimately, impairment of directed cell migration. Moreover, the absence of *Sall1* increased podocyte apoptosis following ADR treatment. GRP78 expression was higher in ADR-treated *Sall1* KO$^{Pod\circ/Pod\circ}$ mice than in control mice. Thus, in injured podocytes, *Sall1* expression protects podocytes via stabilization of synaptopodin and by reducing ER stress through increasing GRP78 expression.

We observed that *Sall1* expression is rarely detected in mature glomeruli; however, this does not mean that *Sall1* is not present. *Sall1*-expressing cells proliferate following ischemia-reperfusion injury,[29] that is, ischemic injury increases *Sall1* expression which is very little in adult kidney. In Northern blot analysis, the highest level of *Sall1* mRNA expression in all adult tissues has been observed in human kidney.[30] These results indicate *Sall1* exists at the mRNA level in adult kidney, and *Sall1* expression increases only after podocyte injury.

Podocyte FP effacement and SD disruption in podocyte injury-induced podocyte loss from the GBM are well-known contributors to the progression of glomerulosclerosis.[1,31,32] Podocyte hypertrophy is an initial response to podocyte loss and is an attempt by the cell, which is relatively incapable of proliferating, to cover the underlying GBM in denuded areas where neighboring cells have detached or died.[33] However,

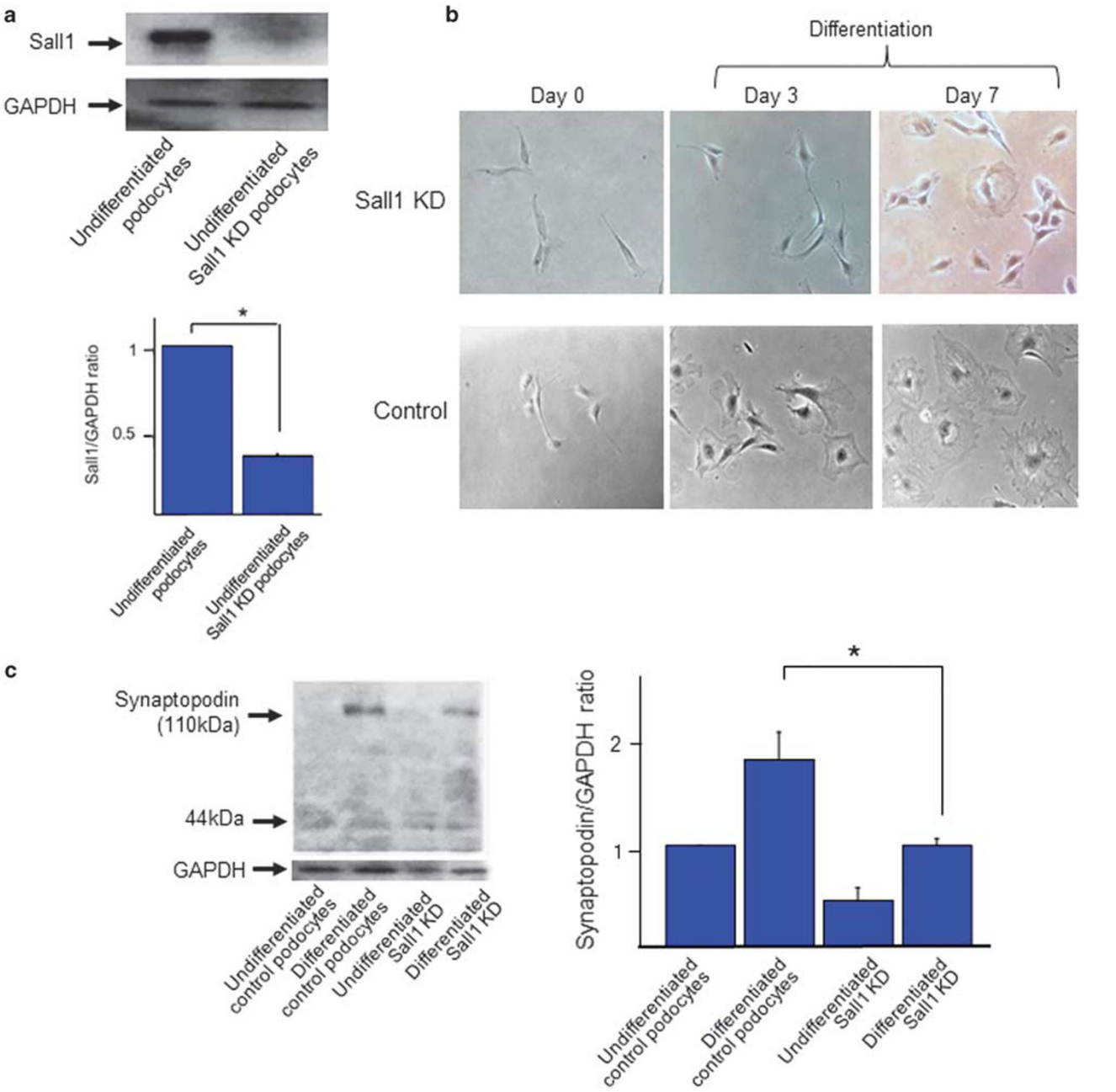

Figure 6 Knockdown (KD) of *Sall1* in cultured podocytes results in loss of actin stress fiber formation, impairment of cell migration, and induction of apoptosis with ADR treatment. (**a**) Western blot analysis of *Sall1* was performed after gene silencing of *Sall1* by stable expression of a specific siRNA in undifferentiated podocytes. *Sall1* KD podocytes exhibit nearly complete loss of the Sall1 protein (*$P<0.05$; $n=5$). (**b**) Differentiated control podocytes exhibit expanded cell bodies with an arborized appearance. In contrast, the cell bodies scarcely expanded under in differentiated *Sall1* KD podocytes (original magnification, 600×). (**c**) Western blot analysis shows that synaptopodin expression (110 kDa) was not detectable in undifferentiated control or *Sall1* KD podocytes. In differentiated *Sall1* KD podocytes, synaptopodin expression is significantly lower than in control differentiated podocytes. Synaptopodin degradation (44 kDa) did not differ between test and control cells (*$P<0.05$). (**d**) IF microscopy shows that synaptopodin was localized in a typical stress fiber–associated pattern in differentiated control podocytes. Fewer stress fibers are present in differentiated *Sall1* KD podocytes (original magnification, 1000×). (**e**) Wound-healing assay. In differentiated *Sall1* KD podocytes, wound closure is significantly delayed at 24 h. Compared with differentiated control podocytes, *Sall1* KD podocytes exhibit significantly impaired directed cell migration (++$P<0.01$). (**f**) Cell migration assay. Compared with differentiated control podocytes, differentiated *Sall1* KD podocytes exhibit significantly impaired motility in migration experiments (*$P<0.05$). (**g**) Analysis of annexin V/PI double-positive populations (late apoptotic cells) and annexin V-positive (PI negative) populations (early apoptotic cells) in cultured differentiated control and *Sall1* KD podocytes after treatment with 0.15 μg/ml of ADR for 48 h. Treatment with ADR induces significant podocyte apoptosis in *Sall1* KD podocytes (*$P<0.01$; $n=5$).

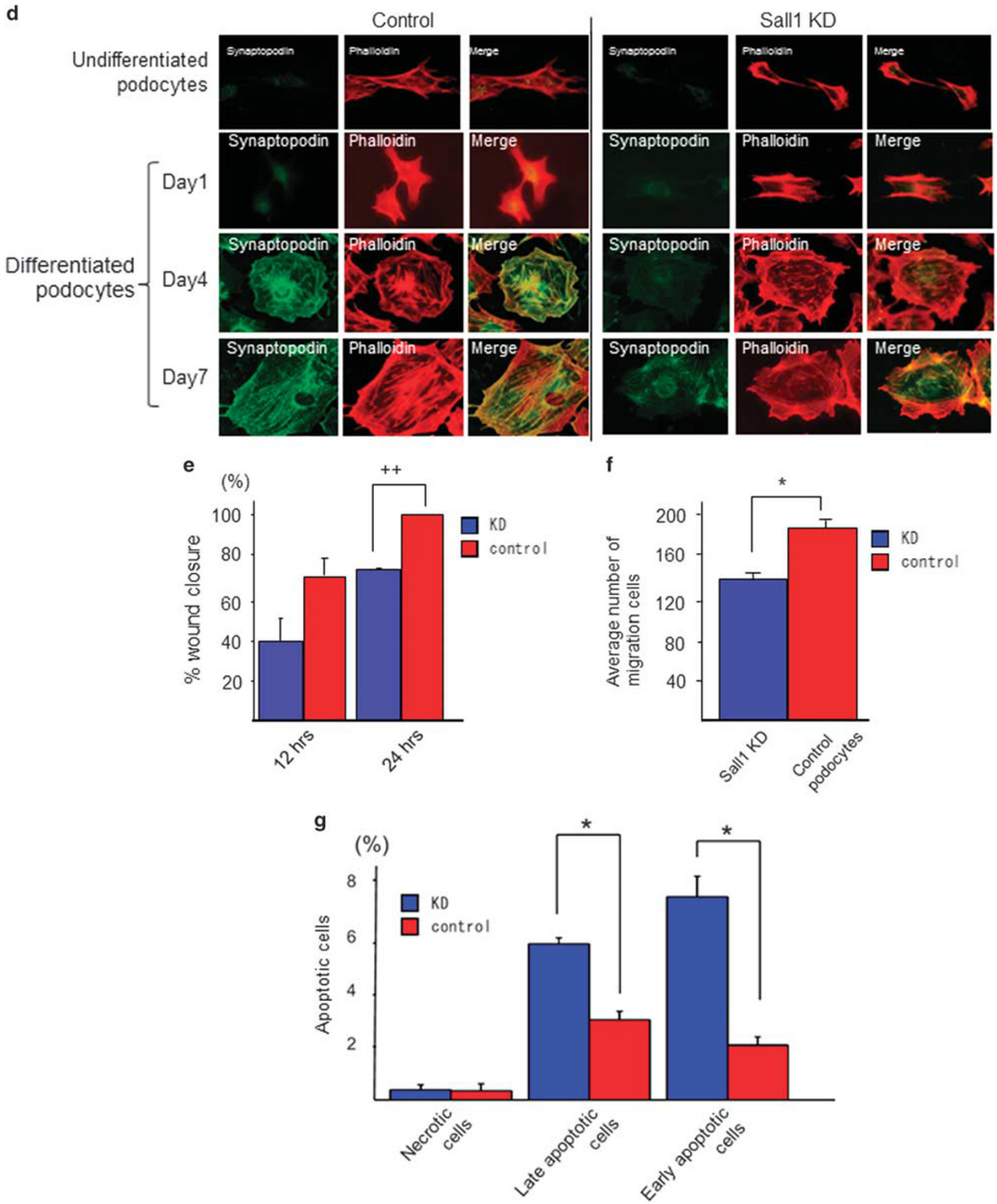

Figure 6 Continued.

several studies also have suggested that prolonged treatment with angiotensin-converting enzyme inhibitors increases the number of podocytes in the absence of podocyte hypertrophy; this event is accompanied by and likely underlies the regression of glomerulosclerosis.[34–36] Our findings are consistent with these observations.

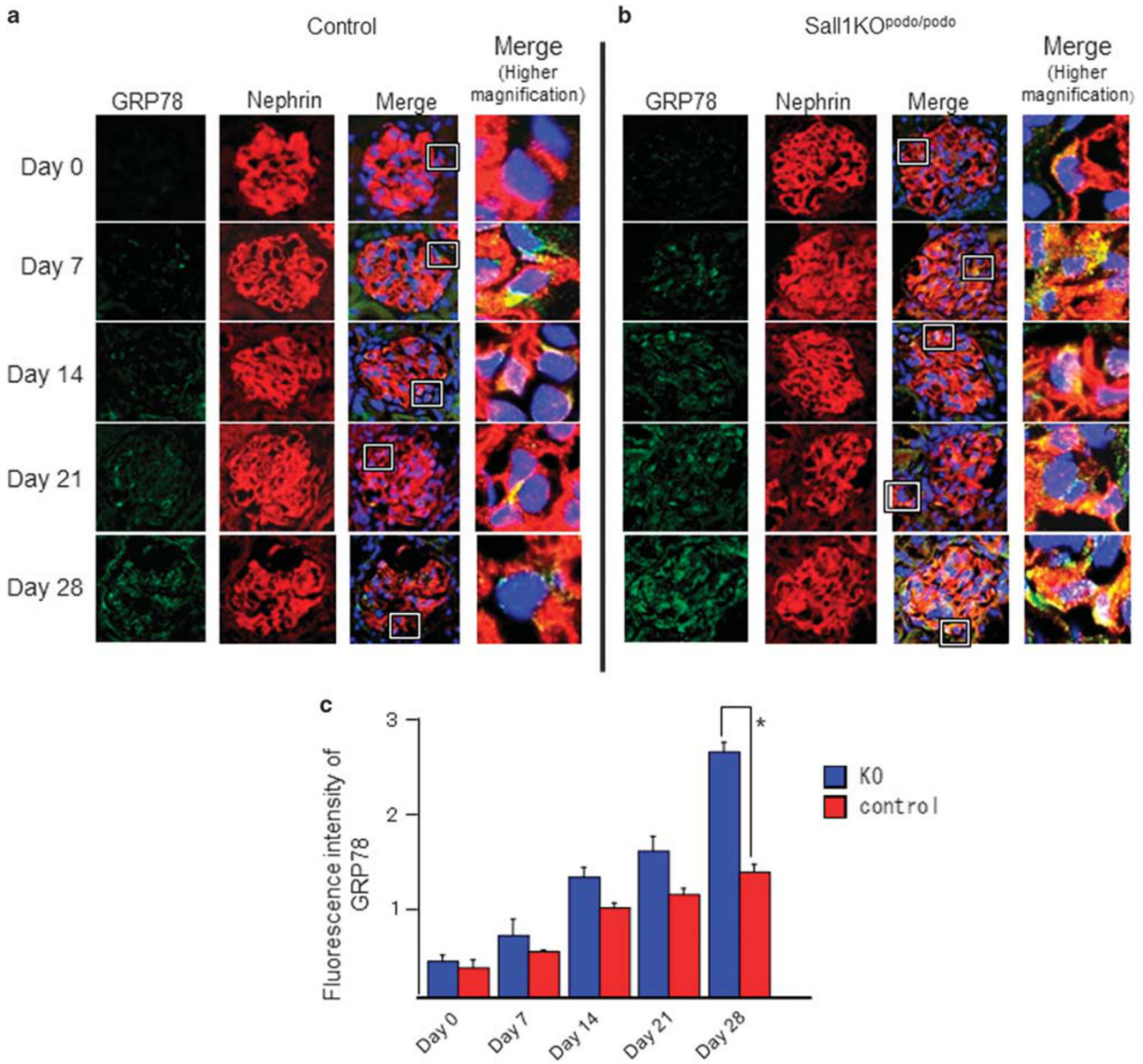

Figure 7 ER stress increased in ADR-injected *Sall1* KO$^{podo/podo}$ mice, as determined by immunofluorescence staining of the ER stress marker GRP78. (**a**) In the ADR-injected control mice, detection of GRP78 expression began on day 7 and slowly increased until day 28. (**b**) In ADR-injected *Sall1* KO$^{podo/podo}$ mice, increased GRP78 expression began on day 7 and persisted until day 28. (**c**) Fluorescence intensity of GRP78. On day 28, the intensity of GRP78 fluorescence was significantly elevated in *Sall1* KO$^{podo/podo}$ mice (*$P<0.05$; $n=5$) (original magnifications: lower, 600×; higher, 1000×).

Mutations affecting several podocyte proteins, including nephrin, podocin, α-actinin4, and synaptopodin, lead to renal disease owing to disruption of the SD and rearrangement of the actin cytoskeleton.[27,37–39] Synaptopodin is essential for the integrity of the podocyte actin cytoskeleton and for the regulation of podocyte cell migration.[24] In the present study, we observed that the loss of *Sall1* induces podocyte loss, increased proteinuria, an increased number of sclerotic glomeruli, and aggregation of actin filaments of FP in ADR-injected *Sall1* KO$^{podo/podo}$ mice. In addition, differentiated *Sall1* KD podocytes showed loss of synaptopodin and suppressed stress fiber formation, ultimately leading to impaired directed cell migration *in vitro*. These results suggest that *Sall1* regulates reorganization of the actin cytoskeleton by upregulating the expression of synaptopodin in injured podocytes and contributes to recovery from podocyte injury. During kidney development, synaptopodin is absent in the early stages of glomerular development, during which the presumptive podocytes display a cortical actin cytoskeleton characteristic of epithelial cells.[20,40] Expression of synaptopodin commences during the subsequent capillary loop stage, when podocytes start developing FP with characteristic

actin-based contractility. Thus, Sall1 may be required for this initial key step of synaptopodin production. To increase synaptopodin protein levels, *Sall1* either directly promotes synaptopodin expression or is associated with a pathway that suppresses synaptopodin degradation. The degradation of synaptopodin is known to cause major reorganization of the actin cytoskeleton, FP effacement, and proteinuria.[24,41] In our experiments, synaptopodin degradation did not increase in *Sall1* KD podocytes, indicating that *Sall1* may directly promote synaptopodin expression.

Several groups have shown that apoptosis is a major cause of podocyte loss from the GBM, leading to proteinuria and glomerulosclerosis.[1,42] In the *in vivo* experiments in the present study, the loss of *Sall1* increased the number of apoptotic podocytes in ADR-injected *Sall1* KO$^{pod\text{-}/pod\text{-}}$ mice. *In vitro*, knockdown of *Sall1* significantly increased the apoptotic damage in ADR-treated podocytes. In *Sall1* KO$^{pod\text{-}/pod\text{-}}$ mice, the number of apoptotic cells was significantly elevated before ADR treatment as compare to WT mice, but the level of cleaved caspase 3 was elevated even before ADR treatment. There are several explanations as to why *Sall1* KO$^{pod\text{-}/pod\text{-}}$ mice or Sall1 KD podocytes exhibit podocyte loss and apoptosis, respectively. *Sall1* might directly regulate podocyte apoptosis. In podocytes, Smad7 a transcription factor that mediates transforming growth factor-β (TGFβ)-induced apoptosis.[43] By contrast, the activation of cytoplasmic and nuclear estrogen receptors, which induces the transcription of genes encoding mitochondrial proteins, significantly protects podocytes against apoptosis.[44] Thus, Sall1 may be the first transcription factor found to have a protective role against podocyte apoptosis.

In the present study, cleaved caspase 3 was not detected in the isolated glomeruli of ADR-injected *Sall1* KO$^{pod\text{-}/pod\text{-}}$ mice as detected in ADR-treated *Sall1* KD podocytes. In *Sall1* KO$^{pod\text{-}/pod\text{-}}$ mice, the ADR-injured podocytes may have already detached from the glomeruli by day 28 during apoptosis.

The ER stress marker GRP78 is a key protein in the pathogenesis of some kidney diseases. In the present study, GRP78 expression was induced by ADR injection in controls and *Sall1* KO$^{pod\text{-}/pod\text{-}}$ mice, with elevated expression in *Sall1* KO$^{pod\text{-}/pod\text{-}}$ mice. Yuan *et al* recently demonstrated that GRP78 knockdown increased RhoA activity and decreased Rac activity in MiaPaCa-2 cells.[45] In contrast, GRP78 overexpression in Capan-2 cells resulted in decreased RhoA and increased Rac activity. GRP78 knockdown cells also exhibited significantly increased numbers of stress fibers. Considering these results, the increased expression of GRP78 observed in this study would cause a decrease in actin bundles in *Sall1* KO$^{pod\text{-}/pod\text{-}}$ mice. Liu *et al* also demonstrated that the expression of synaptopodin and GRP78 in podocytes correlated negatively with proteinuria.[46] As demonstrated in our previous study, synaptopodin controls RhoA expression.[24] These results suggest that GRP78 upregulation and synaptopodin downregulation suppresses RhoA expression and greatly decreases the number of stress fibers and actin bundles. This fragile condition correlates with apoptosis, which is related to the degradation of synaptopodin and ER stress.

In this study, we demonstrate GRP78 upregulation in ADR-injected *Sall1* KO$^{pod\text{-}/pod\text{-}}$ mice and synaptopodin downregulation in *Sall1* KD podocytes. These results indicate that the loss of Sall1 in podocytes increases ER stress and apoptosis and abrogates stress fiber formation. In summary, Sall1 may have a renoprotective effect by contributing to the process of podocyte recovery from injury.

Supplementary Information accompanies the paper on the Laboratory Investigation website (http://www.laboratoryinvestigation.org)

ACKNOWLEDGMENTS

We thank Prof. Lawrence B. Holzman (University of Pennsylvania) for the *podocin-Cre* mice. We thank the Laboratory of Molecular and Biochemical Research, the Research Support Center, Ms. Terumi Shibata, Ms. Taeko Ikuhara, Ms. Izumi Taki, Ms. Kaori Takahashi, Mr Junichi Nakamoto, and Mr Mitsutaka Yoshida, Juntendo University Graduate School of Medicine, Tokyo, Japan, for their excellent technical assistance. This work was supported by research grants from the Kanae Foundation for the Promotion of Medical Science and Kowa Life Science Foundation to KA, by a research assistant grant from the Research Institute for Diseases of Old Age to YH-N and JAOT, by a Grant-in-Aid for Challenging Exploratory Research: (20380058) to KA, by a Grant-in-Aid for Young Scientists (B): (21790821) (23790955) to EA, by a Grant-in-Aid for Young Scientists (B): (24790858) to FK, by a Grant-in-Aid for Young Scientists (B): (24790856) to MT, by a Grant-in-Aid for Young Scientists (B): (23790956) to TH, and by a Grant-in-Aid for Young Scientists (B): (26860648) to YH-N. This work was supported by the program for women researchers from Juntendo University in 2016 funded by the 'Initiative for Realizing Diversity in the Research Environment' from MEXT, Japan. Unrelated to this study, Katsuhiko Asanuma has received research funding from the Mitsubishi Tanabe Pharmaceutical Corporation. We would like to thank Enago (www.enago.jp) for the English language review.

DISCLOSURE/CONFLICT OF INTEREST

The authors declare no conflict of interest.

1. Mundel P, Shankland SJ. Podocyte biology and response to injury. J Am Soc Nephrol 2002;13:3005–3015.
2. Kühnlein RP, Frommer G, Friedrich M, *et al.* Spalt encodes an evolutionarily conserved zinc finger protein of novel structure which provides homeotic gene function in the head and tail region of the Drosophila embryo. EMBO J 1994;13:168–179.
3. Kohlhase J, Altmann M, Archangelo L, *et al.* Genomic cloning, chromosomal mapping, and expression analysis of msal-2. Mamm Genome 2000;11:64–68.
4. Yamashita K, Sato A, Asashima M, *et al.* Mouse homolog of *SALL1*, a causative gene for townes-brocks syndrome, binds to A/T-rich sequences in pericentric heterochromatin via its C-terminal zinc finger domains. Genes Cells 2007;12:171–182.
5. Lauberth SM, Rauchman M. A conserved 12-amino acid motif in *Sall1* recruits the nucleosome remodeling and deacetylase corepressor complex. J Biol Chem 2006;281:23922–23931.
6. Kohlhase J, Wischermann A, Reichenbach H, *et al.* Mutations in the *SALL1* putative transcription factor gene cause townes-brocks syndrome. Nat Genet 1998;18:81–83.
7. Nishinakamura R, Takasato M. Essential roles of *Sall1* in kidney development. Kidney Int 2005;68:1948–1950.
8. Hosoe-Nagai Y. *Sall1*, an indispensable protein for kidney development, plays a renoprotective role in podocyte injury. Juntendo Med J 2014;60:49–55.
9. Roselli S, Gribouval O, Boute N, *et al.* Podocin localizes in the kidney to the slit diaphragm area. Am J Pathol 2002;160:131–139.

10. Kim YH, Goyal M, Kurnit D, *et al.* Podocyte depletion and glomerulosclerosis have a direct relationship in the PAN-treated rat. Kidney Int 2001;60:957–968.
11. Wharram BL, Goyal M, Gillespie PJ, *et al.* Podocyte depletion causes glomerulosclerosis: diphtheria toxin-induced podocyte depletion in rats expressing human diphtheria toxin receptor transgene. J Am Soc Nephrol 2005;16:2941–2952.
12. Bertani T, Poggi A, Pozzoni R, *et al.* Adriamycin-induced nephrotic syndrome in rats: sequence of pathologic events. Lab Invest 1982;46:16–23.
13. Lee VW, Harris DC. Adriamycin nephropathy: a model of focal segmental glomerulosclerosis. Nephrology 2011;16:30–38.
14. Chen A, Sheu LF, Ho YS, *et al.* Experimental focal segmental glomerulosclerosis in mice. Nephron 1998;78:440–452.
15. Asanuma K, Akiba-Takagi M, Kodama F, *et al.* Dendrin location in podocytes is associated with disease progression in animal and human glomerulopathy. Am J Nephrol 2011;33:537–549.
16. Asanuma K, Campbell KN, Kim K, *et al.* Nuclear relocation of the nephrin and CD2AP-binding protein dendrin promotes apoptosis of podocytes. Proc Natl Acad Sci USA 2007;104:10134–10139.
17. Moeller MJ, Sanden SK, Soofi A, *et al.* Podocyte-specific expression of cre recombinase in transgenic mice. Genesis 2003;35:39–42.
18. Yuri S, Fujimura S, Nimura K, *et al.* Sall4 is essential for stabilization, but not for pluripotency, of embryonic stem cells by repressing aberrant trophectoderm gene expression. Stem Cells 2009;27:796–805.
19. Tanimoto M, Gohda T, Kaneko S, *et al.* Effect of pyridoxamine (K-163), an inhibitor of advanced glycation end products, on type 2 diabetic nephropathy in KK-A(y)/Ta mice. Metabolism 2007;56:160–167.
20. Mundel P, Reiser J, Zúñiga Mejía Borja A, *et al.* Rearrangements of the cytoskeleton and cell contacts induce process formation during differentiation of conditionally immortalized mouse podocyte cell lines. Exp Cell Res 1997;236:248–258.
21. Asanuma K, Kim K, Oh J, *et al.* Synaptopodin regulates the actin-bundling activity of alpha-actinin in an isoform-specific manner. J Clin Invest 2005;115:1188–1198.
22. Omata M, Taniguchi H, Koya D, *et al.* N-acetyl-seryl-aspartyl-lysyl-proline ameliorates the progression of renal dysfunction and fibrosis in WKY rats with established anti-glomerular basement membrane nephritis. J Am Soc Nephrol 2006;17:674–685.
23. Asanuma K, Tanida I, Shirato I, *et al.* MAP-LC3, a promising autophagosomal marker, is processed during the differentiation and recovery of podocytes from PAN nephrosis. FASEB J 2003;17:1165–1167.
24. Asanuma K, Yanagida-Asanuma E, Faul C, *et al.* Synaptopodin orchestrates actin organization and cell motility via regulation of RhoA signalling. Nat Cell Biol 2006;8:485–491.
25. Zollinger HU, Mihatsch MJ. Renal Pathology in Biopsy. Springer-Verlag: New York, 1978, p 64.
26. Kusano T, Takano H, Kang D, *et al.* Endothelial cell injury in acute and chronic glomerular lesions in patients with IgA nephropathy. Hum Pathol 2016;49:135–144.
27. Yanagida-Asanuma E, Asanuma K, Kim K, *et al.* Synaptopodin protects against proteinuria by disrupting Cdc42:IRSp53:Mena signaling complexes in kidney podocytes. Am J Pathol 2007;171: 415–427.
28. Nakajo A, Khoshnoodi J, Takenaka H, *et al.* Mizoribine corrects defective nephrin biogenesis by restoring intracellular energy balance. J Am Soc Nephrol 2007;18:2554–2564.
29. Abedin MJ, Imai N, Rosenberg ME, *et al.* Identification and characterization of Sall1-expressing cells present in the adult mouse kidney. Nephron Exp Nephrol 2011;119:e75–e82.
30. Kohlhase J, Schuh R, Dowe G, *et al.* Isolation, characterization, and organ-specific expression of two novel human zinc finger genes related to the drosophila gene spalt. Genomics 1996;38:291–298.
31. Pagtalunan ME, Miller PL, Jumping-Eagle S, *et al.* Podocyte loss and progressive glomerular injury in type II diabetes. J Clin Invest 1997;99: 342–348.
32. Faul C, Asanuma K, Yanagida-Asanuma E, *et al.* Actin up: regulation of podocyte structure and function by components of the actin cytoskeleton. Trends Cell Biol 2007;17:428–437.
33. Lasagni L, Lazzeri E, Shankland SJ, *et al.* Podocyte mitosis—a catastrophe. Curr Mol Med 2013;13:13–23.
34. Remuzzi G, Benigni A, Remuzzi A. Mechanisms of progression and regression of renal lesions of chronic nephropathies and diabetes. J Clin Invest 2006;116:288–296.
35. Macconi D, Sangalli F, Bonomelli M, *et al.* Podocyte repopulation contributes to regression of glomerular injury induced by ACE inhibition. Am J Pathol 2009;174:797–807.
36. Gagliardini E, Corna D, Zoja C, *et al.* Unlike each drug alone, lisinopril if combined with avosentan promotes regression of renal lesions in experimental diabetes. Am J Physiol Renal Physiol 2009;297:F1448–F1456.
37. Oh J, Reiser J, Mundel P. Dynamic (re)organization of the podocyte actin cytoskeleton in the nephrotic syndrome. Pediatr Nephrol 2004;19:130–137.
38. Tryggvason K, Patrakka J, Wartiovaara J. Hereditary proteinuria syndromes and mechanisms of proteinuria. N Engl J Med 2006;354:1387–1401.
39. Durvasula RV, Shankland SJ. Podocyte injury and targeting therapy: an update. Curr Opin Nephrol Hypertens 2006;15:1–7.
40. Mundel P, Heid HW, Mundel TM, *et al.* Synaptopodin: an actin-associated protein in telencephalic dendrites and renal podocytes. J Cell Biol 1997;139:193–204.
41. Faul C, Donnelly M, Merscher-Gomez S, *et al.* The actin cytoskeleton of kidney podocytes is a direct target of the antiproteinuric effect of cyclosporine A. Nat Med 2008;14:931–938.
42. Hendry BM, Khwaja A, Qu QY, *et al.* Distinct functions for Ras GTPases in the control of proliferation and apoptosis in mouse and human mesangial cells. Kidney Int 2006;69:99–104.
43. Schiffer M, Bitzer M, Roberts IS, *et al.* Aptosis in podocytes induced by TGF-beta and Smad7. J Clin Invest 2001;108:807–816.
44. Kummer S, Jeruschke S, Wegerich LV, *et al.* Estrogen receptor alpha expression in podocytes mediates protection against apoptosis in-vitro and in-vivo. PLoS One 2011;6:e27457.
45. Yuan XP, Dong M, Li X, *et al.* GRP78 promotes the invasion of pancreatic cancer cells by FAK and JNK. Mol Cell Biochem 2015;398: 55–62.
46. Liu YJ, Wen YB, Tao JL, *et al.* Correlations of podocyte injury with glucose regulated protein 78 expression and proteinuria in patients with diabetic nephropathy. Zhongguo Yi Xue Ke Xue Yuan Xue Bao 2012;34:359–363.